Mechanics of Materials 56 (2013) 23–37

Contents lists available at SciVerse ScienceDirect

Mechanics of Materials

journal homepage: www.elsevier.com/locate/mechmat

Derivation of strain gradient length via homogenization of heterogeneous elastic materials

Antonios Triantafyllou [a,b], Antonios E. Giannakopoulos [b,*]

[a] Laboratory of Reinforced Concrete Technology and Structures, Department of Civil Engineering, University of Thessaly, Volos 38334, Greece
[b] Laboratory for Strength of Materials and Micromechanics, Department of Civil Engineering, University of Thessaly, Volos 38334, Greece

ARTICLE INFO

Article history:
Received 31 October 2011
Received in revised form 6 June 2012
Available online 27 September 2012

Keywords:
Strain gradient elasticity
Homogenization
Mechanical properties

ABSTRACT

We present explicit upper bound estimates of the microstructural length used in simple gradient elasticity. Our model is a two dimensional composite made of circular hard inclusions randomly dispersed in a soft matrix. Both inclusions and matrix are described by isotropic linear elastic constitutive laws. The composite, however, is described by an isotropic gradient elastic law. The elastic modulus and the Poisson's ratio are given by the exact classic analysis of Christensen. The in-plane microstructural length is estimated by energy optimization, based on solutions of the gradient elastic hollow cylinder. It was shown that the microstructural length decreases with the composition of the particles, taking high values at low particle composition. Naturally, the microstructural length is proportional to the particle diameter and increases with the stiffness of the particles. It was shown that there can be no microstructural prediction for particles that are softer than the matrix. This interesting result seems to be complementary to the result of Bigoni and Drugan who found that, for the couple-stress composite model, there can be no prediction for the microstructural length when the particles are stiffer than the matrix.

1. Introduction

The novelty of gradient elasticity theories is the inclusion of an intrinsic length parameter or internal length in the constitutive equations that describe the mechanical behavior of the material. The inclusion of this new parameter allows these theories to explain the size effect that has been shown experimentally to exist in heterogeneous materials. The two simplest and well studied gradient elasticity theories are the couple stress elasticity (or constraint Cosserat theory) (Mindlin and Tiersten, 1962; Koiter, 1964) and the dipolar elasticity theory (or grade-two theory) (Toupin, 1962; Mindlin, 1964). The main difference between the two is that in the strain-energy density function that they assume: the first associates the internal length with the gradient of the rotations, whereas the second with the gradient of the strains. However, in both theories the internal length is associated with the microstresses that are developed due to the microstructure of the material. In the present work, we employ the simplest possible dipolar model of just one additional length parameter. This choice is based on the fact that one length parameter is enough for predicting size effect and furthermore models with more internal lengths are both unpractical and difficult to verify experimentally.

A typical composite material consists of a matrix and inclusions. The macroscopic material properties of the composite depend on the individual properties of these two phases. The aim of homogenization is to replace the composite material with an equivalent material of uniform macroscopic properties. Micro-mechanical models have been developed for both cases of particulate and fiber reinforcement. Among the many homogenization methods that have been proposed are the Mori–Tanaka method

* Corresponding author. Tel.: +30 24210 74179; fax: +30 24210 74169.
E-mail address: agiannak@uth.gr (A.E. Giannakopoulos).

0167-6636/$ - see front matter © 2012 Elsevier Ltd. All rights reserved.
http://dx.doi.org/10.1016/j.mechmat.2012.09.007

(Mori and Tanaka, 1973), the Self Consistent method (Budiansky, 1965; Hill, 1965), the Generalized Self Consistent method (Christensen and Lo, 1979) and the Differential method (McLaughlin, 1977; Norris, 1985). All these methods aim at deriving the material properties of elasticity which in the case of isotropy are the modulus of elasticity and the Poisson ratio. However, when gradient theories are considered, an additional material parameter, the internal length, must be added. Nevertheless, the same strategy of homogenization can be used, only this time, to yield an estimate for this new parameter.

In the present paper, the elastic energy of the heterogeneous Cauchy-elastic material will be compared with that of the homogeneous strain gradient elastic material and the characteristic length will be estimated as function of the inclusion radius, volume fraction and elastic constants. The analysis will be limited to the two-dimensional (2D) case of circular inclusions.

The paper is structured as follows: In Section 2 we present the classic results for the in-plane effective elastic moduli (the shear modulus μ and the Poisson's ratio v). In Section 3 we present the elastic energies for the various composite cylinder cases. In Section 4 we present the gradient elasticity solutions for the corresponding composite problem. In Section 5 we give the methodology for the estimation of the internal length and some important remarks concerning the model are given in Section 6. Finally in Section 7, we apply our model to an example of steel fiber reinforced concrete mixture and we compare our estimate with the only other model in the literature that predicts the strain gradient internal length parameter.

2. Effective material properties of transversely isotropic composites

The following relationships for the effective material properties are derived with the generalized self consistent method for the specific case cylindrical inclusions, as predicted in Christensen (1990). It is noted that the subscript m stands for the heterogeneous matrix material and the subscript i stands for the inclusion. The symbols without subscript are the effective material properties of the homogeneous material. The overall elastic behavior is that of a transversely isotropic homogeneous material, requiring five material constants: two of them (μ, v) describe the isotropy of the plane (x_2, x_3) which is of interest in this paper.

The in-plane shear modulus μ, is given by:

$$A\left(\frac{\mu}{\mu_m}\right)^2 + 2B\left(\frac{\mu}{\mu_m}\right) + C = 0 \tag{2.1}$$

with

$$\begin{aligned} A &= 3c(1-c)^2\left(\frac{\mu_i}{\mu_m}-1\right)\left(\frac{\mu_i}{\mu_m}+n_i\right) \\ &\quad + \left[\frac{\mu_i}{\mu_m}n_m + n_m n_i - \left(\frac{\mu_i}{\mu_m}n_m - n_i\right)c^3\right] \\ &\quad \times \left[cn_m\left(\frac{\mu_i}{\mu_m}-1\right) - \left(\frac{\mu_i}{\mu_m}n_m + 1\right)\right] \end{aligned}$$

$$\begin{aligned} B &= -3c(1-c)^2\left(\frac{\mu_i}{\mu_m}-1\right)\left(\frac{\mu_i}{\mu_m}+n_i\right) \\ &\quad + \frac{1}{2}\left[n_m\frac{\mu_i}{\mu_m} + \left(\frac{\mu_i}{\mu_m}-1\right)c + 1\right] \\ &\quad \times \left[(n_m-1)\left(\frac{\mu_i}{\mu_m}+n_i\right) - 2\left(\frac{\mu_i}{\mu_m}n_m - n_i\right)c^3\right] \\ &\quad + \frac{c}{2}(n_m+1)\left(\frac{\mu_i}{\mu_m}-1\right)\left[\frac{\mu_i}{\mu_m}+n_i + \left(\frac{\mu_i}{\mu_m}n_m - n_i\right)c^3\right] \end{aligned} \tag{2.2}$$

$$\begin{aligned} C &= 3c(1-c)^2\left(\frac{\mu_i}{\mu_m}-1\right)\left(\frac{\mu_i}{\mu_m}+n_i\right) \\ &\quad + \left[n_m\frac{\mu_i}{\mu_m} + \left(\frac{\mu_i}{\mu_m}-1\right)c + 1\right] \\ &\quad \times \left[\frac{\mu_i}{\mu_m}+n_i + \left(\frac{\mu_i}{\mu_m}n_m - n_i\right)c^3\right] \end{aligned}$$

$$\begin{aligned} n_m &= 4 - 3v_m \\ n_i &= 4 - 3v_i \end{aligned} \tag{2.3}$$

where c is the volume fraction of the inclusions and v denotes the Poisson ratio.

The in-plain bulk modulus K is:

$$K = K_m + \frac{\mu_m}{3} + \frac{c}{\frac{1}{K_i - K_m + (1/3)(\mu_i - \mu_m)} + \frac{1-c}{K_m + (4/3)\mu_m}} \tag{2.4}$$

The axial modulus E_1 (in the x_1 direction, normal to the (x_2, x_3) plane) is:

$$E_1 = cE_i + (1-c)E_m + \frac{4c(1-c)(v_i - v_m)^2\mu_m}{(1-c)\left(\frac{\mu_m}{K_i+\mu_i/3}\right) + c\left(\frac{\mu_m}{K_m+\mu_m/3}\right) + 1} \tag{2.5}$$

The axial Poisson ratio v_1 is:

$$v_1 = cv_i + (1-c)v_m + \frac{c(1-c)(v_i - v_m)\left[\frac{\mu_m}{K_m+\mu_m/3} - \frac{\mu_m}{K_i+\mu_i/3}\right]}{(1-c)\left(\frac{\mu_m}{K_i+\mu_i/3}\right) + c\left(\frac{\mu_m}{K_m+\mu_m/3}\right) + 1} \tag{2.6}$$

The in-plain Poisson ratio, v, is given by Hashin and Rosen (1964):

$$v = \frac{K - \psi\mu}{K + \psi\mu} \tag{2.7}$$

where

$$\psi = 1 + \frac{4Kv_1^2}{E_1} \tag{2.8}$$

The above solution can be simplified for the two extreme cases of rigid inclusions and porous materials. The limiting case of a porous material can be derived directly from the general case represented by (2.2)–(2.8), if we set $\mu_i = v_i = 0$.

For the case of fibers much stiffer than the matrix, only the coefficients of the μ_i terms in A, B, C of (2.2) need be retained with the other being vanishing small. Hence, the A, B, C coefficients, when inclusions are much stiffer than the matrix, take the form:

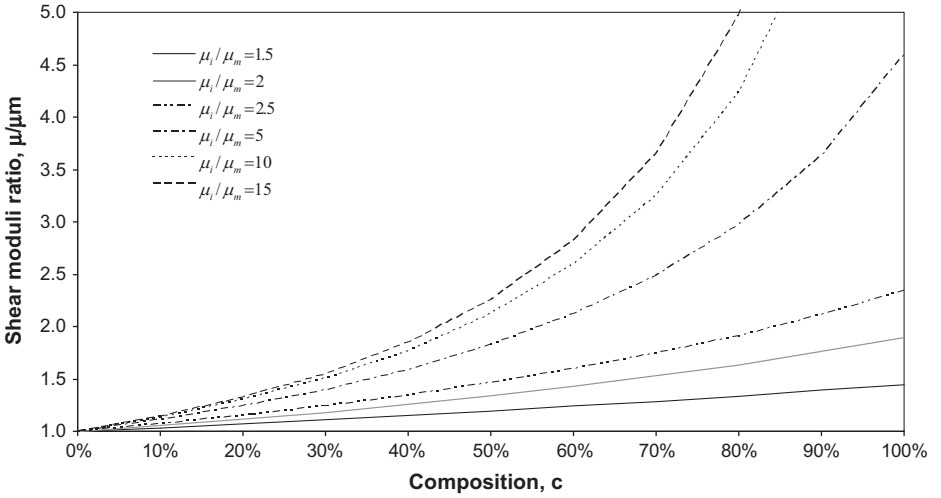

Fig. 1. Effective shear modulus ratios for the case of elastic cylindrical inclusion for various inclusions to matrix shear modulus ratio ($\mu_i/\mu_m = 1.5, 2, 2.5, 5, 10, 15$). Poisson ratio of matrix and inclusion is $\nu_m = 0.2$ and $\nu_i = 0.25$ respectively.

$$\begin{aligned} A &= 3c(1-c)^2 + n_m^2(1-c^3)(c-1) \\ B &= -3c(1-c)^2 + (1/2)(n_m+c)(n_m-1-2n_m c^3) \\ &\quad + (c/2)(n_m+1)(1+n_m c^3) \\ C &= 3c(1-c)^2 + (n_m+c)(1+n_m c^3) \end{aligned} \tag{2.9}$$

The rest of the solution for the case of rigid inclusions is found, if we assume $\mu_i \to \infty$ and modify Eqs. (2.4)–(2.8) accordingly.

These results have been shown to give good estimates not only for the case of dilute composition but also for the limiting case of full packing of the inclusion phase ($c \to 1$). In addition to the physical consistency of the results, it should be noted that the generalized self consistent method is the only complete, exact, closed form solution for the two-dimensional (2D) case of cylindrical inclusions.

The normalized composite shear modulus μ/μ_m of elastic cylindrical inclusions is shown in Fig. 1, allowing the inclusion to matrix shear modulus ratio to range from 1.5 to 15. The assumed matrix and inclusion Poisson ratios for all cases considered are 0.2 and 0.25 respectively.

The limiting cases of rigid fibers and of porous materials are shown in a semi-logarithmic plot in Figs. 2 and 3 respectively. Both results depend (weakly) only on the Poisson ratio of the matrix and four cases are plotted corresponding to matrix Poisson ratios of 0.1, 0.15, 0.2 and 0.25.

A comparison between the three cases is shown in Fig. 4. The matrix Poisson ratio is 0.2 for all cases. The shear modulus ratio for the elastic inclusion case is $\mu_i/\mu_m = 2$. The rigid inclusion and the void solution are upper and lower bounds for μ_i/μ_m respectively.

3. Classic elasticity solutions

The solution of a circular ring under plain strain conditions subjected to normal uniform pressure p applied at the outer boundary $r = b$ and to normal uniform pressure q applied at the inner boundary $r = a$ is (Kachanov et al., 2003; Timoshenko and Goodier, 1951) (see Fig. 5):

$$\begin{aligned} u_r &= \frac{1}{2\mu_m(b^2-a^2)}\left\{b^2a^2(q-p)\frac{1}{r} + (1-2\nu_m)(qa^2-pb^2)r\right\} \\ u_\theta &= 0 \end{aligned} \tag{3.1}$$

$$\begin{aligned} \sigma_{rr} &= \frac{(p-q)b^2a^2}{b^2-a^2}\frac{1}{r^2} + \frac{qa^2-pb^2}{b^2-a^2} \\ \sigma_{\theta\theta} &= -\frac{(p-q)b^2a^2}{b^2-a^2}\frac{1}{r^2} + \frac{qa^2-pb^2}{b^2-a^2} \\ \sigma_{r\theta} &= 0 \end{aligned} \tag{3.2}$$

where u_r is the radial displacement, σ_{rr} the radial stress, $\sigma_{\theta\theta}$ the hoop stress, ν_m the Poisson ratio and μ_m the shear modulus of elasticity. Subscripts r and θ denote radial and circumferential directions of the ring.

The elastic energy is:

$$U_{cl} = 2\pi\int_\alpha^b \frac{r}{2}(\sigma_{rr}\varepsilon_{rr} + \sigma_{\theta\theta}\varepsilon_{\theta\theta})dr \tag{3.3}$$

The expressions for the strains can be found directly from those of the stresses assuming plane strain constitutive equations (Timoshenko and Goodier, 1951). The constitutive relations of the non-zero strains are:

$$\begin{aligned} \varepsilon_{rr} &= \frac{1}{2\mu_m}\{(1-\nu)\sigma_{rr} - \nu\sigma_{\theta\theta}\} \\ \varepsilon_{\theta\theta} &= \frac{1}{2\mu_m}\{(1-\nu)\sigma_{\theta\theta} - \nu\sigma_{rr}\} \end{aligned} \tag{3.4}$$

3.1. Rigid inclusion

The above general solution of the annulus problem can be modified to yield the solution for the case of rigid inclusion of radius a. In this case the displacements at the inner boundary must be zero. By using (3.1) and setting u_r $(r = a) = 0$, we obtain a relation between the inner and

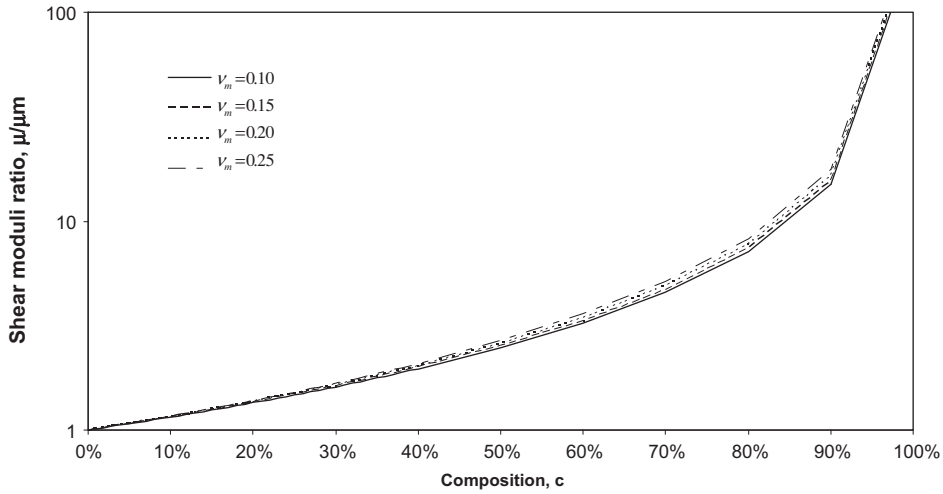

Fig. 2. Effective shear modulus ratio for the case of cylindrical inclusions much stiffer than the matrix for various matrix Poisson ratio values (ν_m = 0.1, 0.15, 0.2, 0.25).

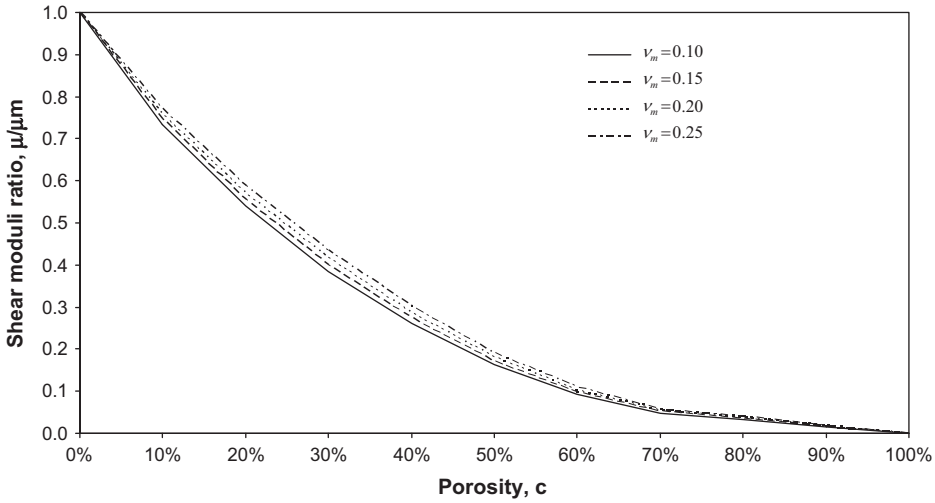

Fig. 3. Effective shear modulus ratio for the case of porous material ($\mu_f = \nu_f = 0$) for various matrix Poisson ratios (ν_m = 0.1, 0.15, 0.2, 0.25).

outer pressures that satisfies this condition. The inner pressure q must be:

$$q = \frac{2b^2(1-\nu_m)p}{b^2 + a^2(1-2\nu_m)} \tag{3.5}$$

If we feed this specific value of q back to (3.1) and (3.2), we will have the solution for the problem of a circular ring containing a rigid inclusion.

The elastic energy U_{cl1} would then be:

$$U_{cl1} = \frac{\pi(1-c)p^2a^2(1-\nu_m-2\nu_m^2)}{2\mu_m(1+\nu_m)c(1+c-2c\nu_m)} \tag{3.6}$$

where c is the composition and is equal to $c = a^2/b^2$ for the 2D case.

We can rearrange (3.6) to become:

$$U_{cl1} = \frac{\pi(1-c)p^2\ell^2\left(\frac{b}{\ell}\right)^2(1-\nu_m-2\nu_m^2)}{2\mu_m(1+\nu_m)(1+c-2c\nu_m)} = \pi \times \ell^2 \times p^2 \times f_1\left(\mu_m, \nu_m, c, \frac{b}{\ell}\right) \tag{3.7}$$

where ℓ is an internal length used to normalize the expression of elastic energy. The addition of this parameter might appear unnecessary at the moment since it does not affect the solution but it will become apparent later.

The first derivative of u_r at $r = b$ is:

$$\left.\frac{\partial u_r}{\partial r}\right|_{r=b} = -\frac{(1+c)p(1-2\nu_m)}{2\mu_m(1+c(1-2\nu_m))} = u^0_{rrr} \tag{3.8}$$

3.2. Porous material (voids)

The general solution for the case of pores is directly obtained from the general results (3.1) and (3.2), if we set $q = 0$. The elastic energy is then:

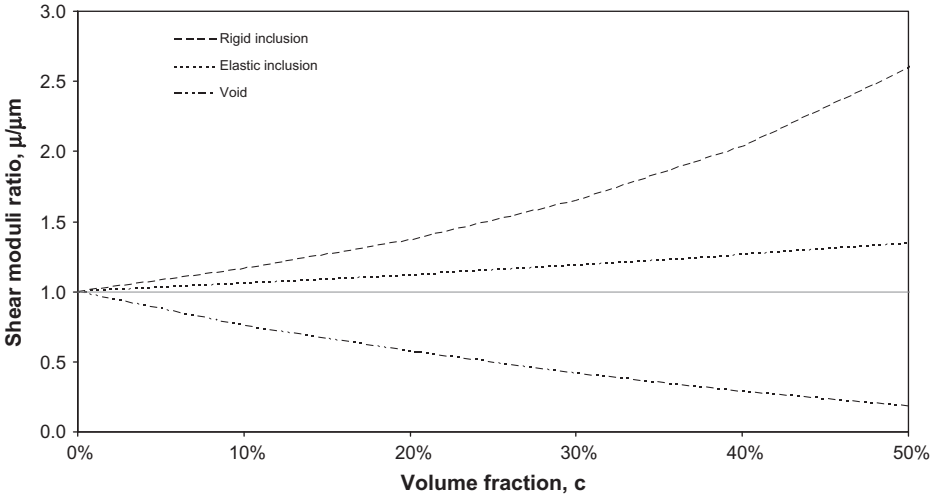

Fig. 4. Comparison between the cases of porous material and elastic matrix material with rigid or elastic inclusions ($\mu_i/\mu_m = 2$) for $\nu_m = 0.2$.

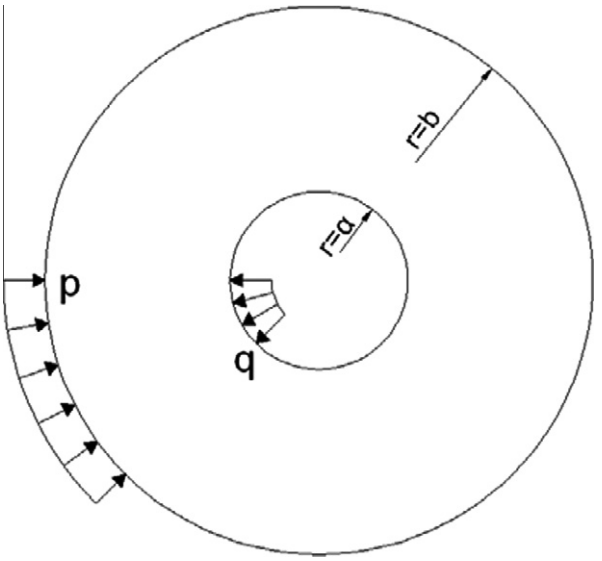

Fig. 5. Circular ring subjected to normal uniform external and internal pressures.

$$U_{cl2} = \frac{\pi p^2 b^2 (1 + c - 2\nu_m)}{2\mu_m (1 - c)} \tag{3.9}$$

and if we normalize the expression of the elastic energy with the internal length ℓ, we obtain:

$$U_{cl2} = \frac{\ell^2 \pi p^2 \left(\frac{b}{\ell}\right)^2 (1 + c - 2\nu_m)}{2\mu_m (1 - c)} = \pi \times \ell^2 \times p^2 \times f_2\left(\mu_m, \nu_m, c, \frac{b}{\ell}\right) \tag{3.10}$$

The first derivative of u_r at $r = b$ is in this case:

$$\left.\frac{\partial u_r}{\partial r}\right|_{r=b} = -\frac{p(1 - c - 2\nu_m)}{2\mu_m (1 - c)} = u^0_{rrr} \tag{3.11}$$

3.3. Elastic inclusions

The solution for this case can be obtained by superimposing the solution of two sub-problems following the well known Eshelby methodology (Eshelby, 1957). We first remove the inclusion and assume an internal pressure q acting at the inner boundary ($r = a$). By solving this problem we obtain the displacement $u(r = a) = u_1$. We then assume a solid circle with the inclusion properties of radius α under normal pressure q. By solving this problem, we obtain the displacement $u(r = a) = u_2$. The two sub-problems are shown in Fig. 6. The solutions to both these problems can be easily obtained from the general solution represented by (3.1) and (3.2) by applying the necessary simplifications for the second sub-problem.

The radial displacement u_1 at $r = a$ of the sub-problem 1, is:

$$u_1 = \frac{a[q(1 + c - 2c\nu_m) - 2p(1 - \nu_m)]}{2\mu_m (1 - c)} \tag{3.12}$$

The radial displacement u_2 at $r = a$ of the sub-problem 2, is:

$$u_2 = -\frac{qa(1 - 2\nu_i)}{2\mu_i} \tag{3.13}$$

The boundary condition of the generic problem demands $u_1 = u_2$. Using (3.12) and (3.13), we obtain the value of q as a function of the outer pressure p and the material properties of the matrix and inclusion. The pressure q must be:

$$q = \frac{2p\mu_i (1 - \nu_m)}{\mu_m (1 - c)(1 - 2\nu_i) + \mu_i (1 + c - 2c\nu_m)} \tag{3.14}$$

If we feed this value of q back to the solution of the two sub-problems, we obtain the solution of the annulus with a circular inclusion.

The elastic energy of the matrix would then be:

$$U_{cl3\_m} = \frac{a^2 (1 - c) p^2 \pi}{2c\mu_m [(1 - c)\mu_m (1 - 2\nu_i) + \mu_i (1 + c - 2c\nu_m)]^2} \times \left[\mu_m^2 (1 - 2\nu_i)^2 (1 + c - 2\nu_m) + 2(1 - c)\mu_i \mu_m (1 - 2\nu_i)(1 - 2\nu_m) + \mu_i^2 (1 - 2\nu_m)(1 + c(1 - 2\nu_m)\right] \tag{3.15}$$

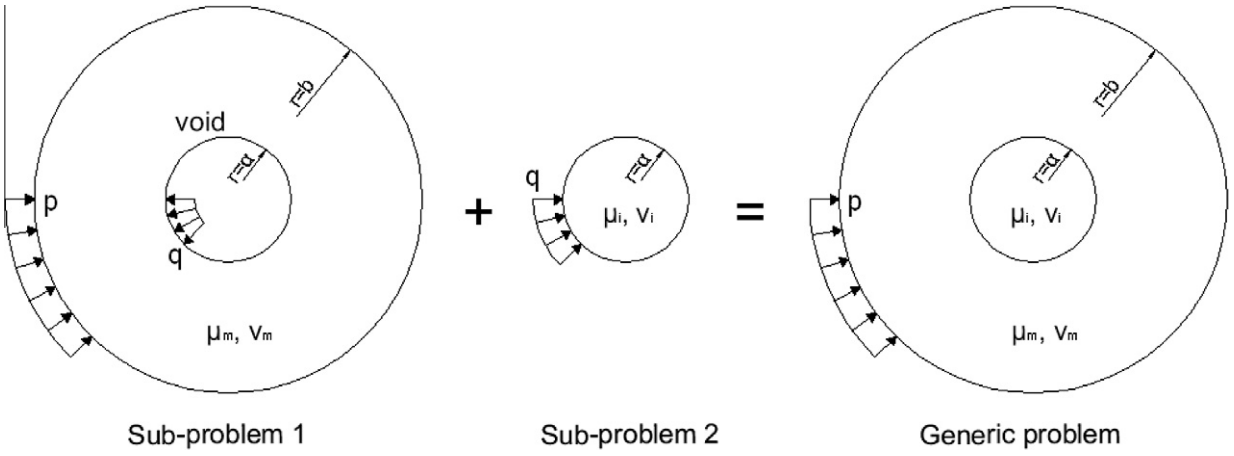

Fig. 6. Superposition of sub-problems 1 and 2 to yield the generic case of an annulus with elastic circular inclusions.

and, if we normalize the expression of the elastic energy with the internal length ℓ, we obtain:

$$\begin{aligned} U_{cl3\_m} &= \frac{\left(\frac{b}{\ell}\right)^2(1-c)p^2\ell^2\pi}{2\mu_m\left[(1-c)\mu_m(1-2\nu_i)+\mu_i(1+c-2c\nu_m)\right]^2} \\ &\times\Big[\mu_m^2(1-2\nu_i)^2(1+c-2\nu_m)+2(1-c)\mu_i\mu_m \\ &(1-2\nu_i)(1-2\nu_m)+\mu_i^2(1-2\nu_m)(1+c(1-2\nu_m)\Big] \\ &= \pi\times\ell^2\times p^2\times f_{3\_m}\left(\mu_m,\nu_m,\mu_i,\nu_i,c,\frac{b}{\ell}\right) \end{aligned} \tag{3.16}$$

The elastic energy of the inclusions is:

$$U_{cl3\_i} = \frac{2a^2p^2\pi\mu_i(1-2\nu_i)(1-\nu_m)^2}{\left[(1-c)\mu_m(1-2\nu_i)+\mu_i(1+c-2c\nu_m)\right]^2} \tag{3.17}$$

and, if we normalize the expression of the elastic energy with the internal length ℓ, we obtain:

$$\begin{aligned} U_{cl3\_i} &= \frac{2c\left(\frac{b}{\ell}\right)^2\ell^2p^2\pi\mu_i(1-2\nu_i)(1-\nu_m)^2}{\left[(1-c)\mu_m(1-2\nu_i)+\mu_i(1+c-2c\nu_m)\right]^2} \\ &= \pi\times\ell^2\times p^2\times f_{3\_i}\left(\mu_m,\nu_m,\mu_i,\nu_i,c,\frac{b}{\ell}\right) \end{aligned} \tag{3.18}$$

Therefore, the total elastic energy of an annulus with an elastic circular inclusion is:

$$\begin{aligned} U_{cl3} &= U_{cl3\_m}+U_{cl3\_i} \\ &= \pi\times\ell^2\times p^2 \\ &\times\left[f_{3\_m}\left(\mu_m,\nu_m,\mu_i,\nu_i,c,\frac{b}{\ell}\right)+f_{3\_i}\left(\mu_m,\nu_m,\mu_i,\nu_i,c,\frac{b}{\ell}\right)\right] \end{aligned} \tag{3.19}$$

and the first derivative of u_r at $r=b$ is:

$$\begin{aligned} \left.\frac{\partial u_r}{\partial r}\right|_{r=b} &= \frac{-p\left[(1+c)\mu_i(1-2\nu_m)+\mu_m(1-2\nu_i)(1-c-2\nu_m\right]}{2\mu_m[(1-c)\mu_m(1-2\nu_i)+\mu_i(1+c-2c\nu_m)]} \\ &= u^0_{rrr} \end{aligned} \tag{3.20}$$

Note that (3.20) gives (3.11) in the case of porous material ($\mu_i=0, \nu_i=0$). Also, in the limit of a rigid inclusion ($\mu_i\to\infty$), (3.20) gives (3.8).

4. Gradient elasticity solution for the annulus problem

Eshel and Rosenfeld (1975) were the first to provide the outline of the gradient elasticity solution for the annulus problem. The problem was solved analytically by Aravas (2011) and Gao and Park (2007) for plain strain conditions. The key points of the solution of the annulus problem (see Fig. 2) are presented below.

The material is an in-plane isotropic, compressible, homogeneous, linear elastic material and is described by an elastic strain energy density function W that incorporates strain gradient effects:

$$W(\varepsilon,\kappa) = \mu\left[\varepsilon_{ij}\varepsilon_{ij}+\frac{\nu}{1-2\nu}\varepsilon_{ij}\varepsilon_{ij}+\ell^2\left(\kappa_{ijk}\kappa_{ijk}+\frac{\nu}{1-2\nu}\kappa_{ijj}\kappa_{ikk}\right)\right] \tag{4.1}$$

where is ℓ is a material length, $\boldsymbol{\varepsilon}$ is the infinitesimal strain tensor and $\boldsymbol{\kappa}$ the strain gradient 3rd order tensor. Note that the deformation in the out-of-plane direction x_3 is zero ($u_3=0$) and also $\varepsilon_{33}=0$, $\kappa_{33k}=0$.

The Cauchy stress and double stress quantities $\boldsymbol{\tau}$ and $\boldsymbol{\lambda}$ are defined as follows:

$$\begin{aligned} \tau_{ij} &= \frac{\partial W}{\partial\varepsilon_{ij}} = 2\mu\left[\varepsilon_{ij}+\frac{\nu}{1-2\nu}\varepsilon_{ij}\delta_{ij}\right] \quad\text{and}\quad \lambda_{ijk} = \frac{\partial W}{\partial\kappa_{ijk}} \\ &= 2\mu\ell^2\left[\kappa_{ijk}+\frac{\nu}{1-2\nu}\kappa_{ipp}\delta_{jk}\right] \end{aligned} \tag{4.2}$$

The following relations also hold true:

$$\boldsymbol{\lambda}=\ell^2\nabla\boldsymbol{\tau}(\lambda_{ijk}=\ell^2\partial\tau_{ij}/\partial x_k) \quad\text{and}\quad \boldsymbol{\kappa}=\nabla\boldsymbol{\varepsilon}(\kappa_{ijk}=\partial\varepsilon_{ij}/\partial x_k) \tag{4.3}$$

The dynamic boundary conditions required by the principal of virtual work, are the Cauchy (P_r) and the double stress tractions (R_r) in the radial direction:

$$\begin{aligned} P_r(r) = \pm\Bigg\{&\frac{c_1}{2}-\frac{c_6}{2r^2}-c_2\frac{\ell}{r}\left[\nu K_1\left(\frac{r}{\ell}\right)-(1-2\nu)K_2\left(\frac{r}{\ell}\right)\right] \\ &+c_3\frac{\ell}{r}\left[\nu I_1\left(\frac{r}{\ell}\right)-(1-2\nu)I_2\left(\frac{r}{\ell}\right)\right]-\frac{c_6}{2}\frac{\ell^2}{r^4}\Bigg\} \end{aligned} \tag{4.4}$$

$$\begin{aligned} R_r(r) = &-c_2\ell\left[(1-\nu)K_1\left(\frac{r}{\ell}\right)+(1-2\nu)K_2\left(\frac{r}{\ell}\right)\right] \\ &+c_3\ell\left[(1-\nu)I_1\left(\frac{r}{\ell}\right)-(1-2\nu)I_2\left(\frac{r}{\ell}\right)\right] \end{aligned} \tag{4.5}$$

where K and I are modified Bessel functions of the first and second kind (the subscript shows the order) and c_1, c_2, c_3 and c_6 are unknown constants to be determined from the following boundary conditions:

$$\begin{aligned} &P_r(a) = -q, \quad R_r(a) = 0 \quad \text{at} \quad r = a \\ &P_r(b) = -p, \quad R_r(b) = 0 \quad \text{at} \quad r = b \end{aligned} \tag{4.6}$$

The radial displacements are:

$$u_r(r) = \frac{1}{2\mu}\left\{\frac{(1-2\nu)c_1}{2}r + \frac{c_6}{2r} - (1-2\nu)\ell \times \left[c_2 K_1\left(\frac{r}{\ell}\right) - c_3 I_1\left(\frac{r}{\ell}\right)\right]\right\} \tag{4.7}$$

and the rest of the solution is:

$$\tau_{rr}(r) = \tau^0_{rr}(r) + \frac{1}{2}\left(c_7 - \frac{c_8}{r^2}\right) + \frac{c_2}{2}\left[K_0\left(\frac{r}{\ell}\right) + (1-2\nu)K_1\left(\frac{r}{\ell}\right)\right] + \frac{c_3}{2}\left[I_0\left(\frac{r}{\ell}\right) + (1-2\nu)I_1\left(\frac{r}{\ell}\right)\right] \tag{4.8}$$

$$\tau_{\theta\theta}(r) = \tau^0_{\theta\theta}(r) + \frac{1}{2}\left(c_7 + \frac{c_8}{r^2}\right) + \frac{c_2}{2}\left[K_0\left(\frac{r}{\ell}\right) - (1-2\nu)K_1\left(\frac{r}{\ell}\right)\right] + \frac{c_3}{2}\left[I_0\left(\frac{r}{\ell}\right) - (1-2\nu)I_1\left(\frac{r}{\ell}\right)\right] \tag{4.9}$$

and

$$\varepsilon_{rr}(r) = \varepsilon^0_{rr}(r) + \frac{1}{2\mu}\left\{\frac{(1-2\nu)}{2}c_7 - \frac{c_8}{2r^2} + (1-2\nu) \times \left\{c_2\left[K_0\left(\frac{r}{\ell}\right) + \frac{\ell}{r}K_1\left(\frac{r}{\ell}\right)\right] + c_3\left[I_0\left(\frac{r}{\ell}\right) - \frac{\ell}{r}I_1\left(\frac{r}{\ell}\right)\right]\right\}\right\} \tag{4.10}$$

$$\varepsilon_{\theta\theta}(r) = \varepsilon^0_{\theta\theta}(r) + \frac{1}{2\mu}\left\{\frac{(1-2\nu)}{2}c_7 + \frac{c_8}{2r^2} - (1-2\nu)\frac{\ell}{r} \times \left[c_2 K_1\left(\frac{r}{\ell}\right) - c_3 I_1\left(\frac{r}{\ell}\right)\right]\right\} \tag{4.11}$$

where τ^0_{rr}, $\tau^0_{\theta\theta}$, ε^0_{rr} and $\varepsilon^0_{\theta\theta}$ represent the classical linear isotropic elasticity solution, (i.e. $\ell = 0$).

$$\tau^0_{rr} = A + \frac{B}{r^2}, \quad \tau^0_{\theta\theta} = A - \frac{B}{r^2} \quad \text{and} \quad u^0_{rr} = \frac{1}{2\mu}\left[(1-2\nu)Ar - \frac{B}{r}\right] \tag{4.12}$$

with

$$A = \frac{qa^2 - pb^2}{b^2 - a^2}, \quad B = (p-q)\frac{a^2 b^2}{b^2 - a^2} \tag{4.13}$$

and

$$c_1 = c_7 + 2A, \quad c_6 = c_8 - 2B \tag{4.14}$$

We are interested in the solution for $a \to 0$. The constants c_2 and c_6 must be zero in order for the displacements to be finite and zero at $r = 0$. Therefore, the unknown constants reduce to just two, c_3 and c_7. However, when trying to calculate the values of these two constants from traction type boundary conditions, they both vanish and the gradient solution reduces to the classical elasticity solution. This is not surprising because in order for the gradient effects to participate in the solution, they must be triggered somehow by the boundary conditions. This is in agreement with the finding of Bigoni and Drugan (2007) who considered corresponding results for Cosserat materials.

In order to overcome this, a kinematic boundary condition is assumed at $r = b$:

$$\left.\frac{\partial u_r}{\partial r}\right|_{r=b} = u^0_{rrr} \tag{4.15}$$

This condition implies that the two dimensional gradient elastic material that represents the composite, assumes a homogeneous gradient of the radial displacement. We will use (4.15) together with the traction type condition $P_r(b) = -p$. In this way we load the gradient material with tractions and displacements gradients that are the same with these of the inhomogeneous classic composite system.

The constants now become:

$$c_8 = c_2 = B = 0, \quad A = -p \tag{4.16}$$

and

$$c_3 = \frac{2b[(1-2\nu)p + 2\mu \times u^0_{rrr}]}{(1-2\nu)\left[b\left(I_0\left(\frac{b}{\ell}\right) + I_2\left(\frac{b}{\ell}\right)\right) - 2\ell\left(I_2\left(\frac{b}{\ell}\right) + \nu I_1\left(\frac{b}{\ell}\right) - 2\nu I_2\left(\frac{b}{\ell}\right)\right)\right]} \tag{4.17}$$

$$c_7 = \frac{-4\ell\left[I_2\left(\frac{b}{\ell}\right) + \nu I_1\left(\frac{b}{\ell}\right) - 2\nu I_2\left(\frac{b}{\ell}\right)\right]\left[(1-2\nu)p + 2\mu \times u^0_{rrr}\right]}{(1-2\nu)\left[b\left(I_0\left(\frac{b}{\ell}\right) + I_2\left(\frac{b}{\ell}\right)\right) - 2\ell\left(I_2\left(\frac{b}{\ell}\right) + \nu I_1\left(\frac{b}{\ell}\right) - 2\nu I_2\left(\frac{b}{\ell}\right)\right)\right]} \tag{4.18}$$

The elastic energy of the gradient solution U_{gr} is:

$$U_{gr} = \pi \int_0^b r(\tau_{rr}\varepsilon_{rr} + \tau_{\theta\theta}\varepsilon_{\theta\theta} + \lambda_{rrr}\kappa_{rrr} + \lambda_{\theta\theta\theta}\kappa_{\theta\theta\theta})dr \tag{4.19}$$

or

$$U_{gr} = \pi\ell^2 \int_0^{b/\ell} \frac{r}{\ell}(\tau_{rr}\varepsilon_{rr} + \tau_{\theta\theta}\varepsilon_{\theta\theta} + \lambda_{rrr}\kappa_{rrr} + \lambda_{\theta\theta\theta}\kappa_{\theta\theta\theta})d\frac{r}{\ell}$$

The values of $\boldsymbol{\kappa}$ and $\boldsymbol{\lambda}$ are obtained after substituting (4.8)–(4.11) into (4.3).

After substituting all the quantities and integrating, the gradient elastic energy becomes:

$$\begin{aligned} U_{gr} = \frac{\pi(-1+2\nu)p^2\ell^2}{4\mu}\Bigg\{ &-\frac{1}{2}\left(\frac{c_7}{p} - 2\right)^2\left(\frac{b}{\ell}\right)^2 - \frac{1}{2}\left(\frac{c_3}{p}\right)^2\left(\frac{b}{\ell}\right)^2 \\ &\times\left[I_0^2\left(\frac{b}{\ell}\right) - I_1^2\left(\frac{b}{\ell}\right)\right] - \frac{1}{2}\left(\frac{c_3}{p}\right)^2\left(\frac{b}{\ell}\right)^2 \\ &\times\left[I_1^2\left(\frac{b}{\ell}\right) - I_0\left(\frac{b}{\ell}\right)I_2\left(\frac{b}{\ell}\right)\right] - \frac{c_3}{p}\left(\frac{c_7}{p} - 2\right)\left(\frac{b}{\ell}\right)^2 \\ &\times HG\Gamma\left[2, \frac{1}{4}\left(\frac{b}{\ell}\right)^2\right] + \frac{1}{2}\left(\frac{c_3}{p}\right)^2\left(-1 + HG\left[\left\{\frac{1}{2}\right\}, \{1,1\}, \left(\frac{b}{\ell}\right)^2\right]\right) \\ &-\left(\frac{c_3}{p}\right)^2\left(-1 + HG\left[\left\{\frac{1}{2}\right\}, \{1,2\}, \left(\frac{b}{\ell}\right)^2\right]\right) \\ &-3\left(\frac{c_3}{p}\right)^2\frac{b}{\ell}(1+2\nu)HG\left[\left\{\frac{1}{2}\right\}, \{2,2\}, \left(\frac{b}{\ell}\right)^2\right] \\ &+\left(\frac{c_3}{p}\right)^2\frac{b}{\ell}(1-2\nu)HG\left[\left\{\frac{1}{2}\right\}, \{2,3\}, \left(\frac{b}{\ell}\right)^2\right] \\ &+2\left(\frac{c_3}{p}\right)^2\frac{b}{\ell}(1-2\nu)HG\left[\left\{\frac{1}{2}, \frac{1}{2}\right\}, \left\{1,1,\frac{3}{2}\right\}, \left(\frac{b}{\ell}\right)^2\right] \\ &-\frac{1}{3}\left(\frac{c_3}{p}\right)^2\left(\frac{b}{\ell}\right)^3(1+2\nu)HG\left[\left\{\frac{3}{2}, \frac{3}{2}\right\}, \left\{2,2,\frac{5}{2}\right\}, \left(\frac{b}{\ell}\right)^2\right] \\ &+\frac{1}{4}\left(\frac{c_3}{p}\right)^2\left(\frac{b}{\ell}\right)^3(1-2\nu)HG\left[\left\{\frac{3}{2}, \frac{3}{2}\right\}, \left\{2,\frac{5}{2},3\right\}, \left(\frac{b}{\ell}\right)^2\right]\Bigg\} \end{aligned} \tag{4.20}$$

or

$$U_{gr} = \pi \times \ell^2 \times p^2 \times g\left(\mu, \nu, c_3, c_7, c, \frac{b}{\ell}\right)$$

where HG is a generalized hypergeometric function and HGΓ is a regularized confluent hypergeometric function (Abramowitz and Stegun, 1970). Both functions are described as:

$$HG[\{a_1,\ldots,a_p\},\{b_1,\ldots,b_q\},x] = {}_pF_q(a;b;x) = \sum_{k=0}^{\infty}(a_1)_k\ldots(a_p)_k/(b_1)_k\ldots(b_q)_k\frac{x^k}{k!}$$

$$HG\Gamma[a,x] = {}_0F_1(a;x)/\Gamma(a),$$

where $\Gamma(\alpha)$ is the Euler gamma function.

Alternatively, the gradient elastic energy can be found from the external work. The elastic energy is then equal to:

$$U_{gr} = \pi b\{P_r(b)u_r(b) + R_r(b)u_r'(b)\} \tag{4.21}$$

where primes denote derivatives with respect to r.

Substituting the value of u^0_{rrr} from (3.20) into (4.17) and (4.18), we can connect the gradient elasticity solutions with the classic elasticity solutions for the three cases of rigid inclusion, porous material and elastic inclusions discussed in Section 3. This approach is similar to that of Bigoni and Drugan (2007) for Cosserat gradient elastic materials. We obtain the constants c_3 and c_7 for each case separately:

For the case of *rigid inclusions* (Fig. 7), the constants become:

$$c_{3\_1} = \frac{2\frac{b}{\ell}p\left[(1-2\nu) - \frac{\mu}{\mu_m}\frac{(1+c)(1-2\nu_m)}{1+c(1-2\nu_m)}\right]}{(1-2\nu)\left[\frac{b}{\ell}\left(I_0\left(\frac{b}{\ell}\right)+I_2\left(\frac{b}{\ell}\right)\right) - 2\left(I_2\left(\frac{b}{\ell}\right)+\nu I_1\left(\frac{b}{\ell}\right) - 2\nu I_2\left(\frac{b}{\ell}\right)\right)\right]} \tag{4.21}$$

$$c_{7\_1} = \frac{-4p\left[I_2\left(\frac{b}{\ell}\right)+\nu I_1\left(\frac{b}{\ell}\right) - 2\nu I_2\left(\frac{b}{\ell}\right)\right]\left[(1-2\nu) - \frac{\mu}{\mu_m}\frac{(1+c)(1-2\nu_m)}{1+c(1-2\nu_m)}\right]}{(1-2\nu)\left[\frac{b}{\ell}\left(I_0\left(\frac{b}{\ell}\right)+I_2\left(\frac{b}{\ell}\right)\right) - 2\left(I_2\left(\frac{b}{\ell}\right)+\nu I_1\left(\frac{b}{\ell}\right) - 2\nu I_2\left(\frac{b}{\ell}\right)\right)\right]} \tag{4.22}$$

For the case of *porous materials* (Fig. 8), the constants become:

$$c_{3\_2} = \frac{2\frac{b}{\ell}p\left[(1-2\nu) - \frac{\mu}{\mu_m}\frac{(1-c-2\nu_m)}{(1-c)}\right]}{(1-2\nu)\left[\frac{b}{\ell}\left(I_0\left(\frac{b}{\ell}\right)+I_2\left(\frac{b}{\ell}\right)\right) - 2\left(I_2\left(\frac{b}{\ell}\right)+\nu I_1\left(\frac{b}{\ell}\right) - 2\nu I_2\left(\frac{b}{\ell}\right)\right)\right]} \tag{4.23}$$

$$c_{7\_2} = \frac{-4p\left[I_2\left(\frac{b}{\ell}\right)+\nu I_1\left(\frac{b}{\ell}\right) - 2\nu I_2\left(\frac{b}{\ell}\right)\right]\left[(1-2\nu) - \frac{\mu}{\mu_m}\frac{(1-c-2\nu_m)}{(1-c)}\right]}{(1-2\nu)\left[\frac{b}{\ell}\left(I_0\left(\frac{b}{\ell}\right)+I_2\left(\frac{b}{\ell}\right)\right) - 2\left(I_2\left(\frac{b}{\ell}\right)+\nu I_1\left(\frac{b}{\ell}\right) - 2\nu I_2\left(\frac{b}{\ell}\right)\right)\right]} \tag{4.24}$$

For the case of *elastic inclusions*(Fig. 9), the constants become:

Note that for all expressions of the constants c_3 and c_7, the internal length appears only in the normalized form b/ℓ. By substituting c_{3_i} and c_{7_i}, with $i = 1, 2, 3$ to (4.20), we obtain three expressions for the gradient elastic energy U_{gr1}, U_{gr2} and U_{gr3} respectively.

5. Estimation of internal length

The energy of the heterogeneous material calculated in Section 3 and the energy of the gradient homogeneous material calculated in Section 4 were determined for the same boundary conditions. By equating the two energies, we can derive an estimation of the internal length of the gradient material as a function of the inclusion radius$a$, the composition ratio c and the elastic material constants of the matrix and the inclusion ($\mu_i/\mu_m, \nu_i, \nu_m$). However, before proceeding, we must face the problem of how to settle the other two material properties of the gradient material which in the general case will not be equal to the matrix material properties. The problem has three unknowns, namely, the internal length ℓ, the in-plane shear modulus μ and the in-plane Poisson ratio ν and we only have one equation to work with, which is:

$$U_{cl} = U_{gr} \tag{5.1}$$

If the solution is limited to dilute concentration of inclusions one can assume that the material properties of the matrix and composite material remain the same. It is noted that the results of Bigoni and Drugan (2007) were derived using this assumption. In this work the two material properties, i.e. the shear modulus and Poisson ratio, were extracted from a classic composite model suitable to our considered problem. By doing so, the unknowns are reduced to just one, the internal length ℓ, which can then be estimated. This approach is justified by the fact that the gradient material should always reduce to the classic material if the gradient effect is neglected, i.e. $\ell = 0$. Therefore the effective material properties predicted by the classical homogenization schemes hold true for the composite gradient material as well. Estimates of the effective material properties of the homogeneous gradient material that correspond to our problem are given in Section 2.

The expression of U_{gr} is highly non-linear and can not be solved explicitly with respect to ℓ. It can however be solved numerically through an iteration process for different values of all the parameters. The solution path is shown

$$c_{3\_3} = \frac{2\frac{b}{\ell}p\left[(1-2\nu) - \frac{\mu\left[(1+c)\mu_i(1-2\nu_m)+\mu_m(1-2\nu_i)(1-c-2\nu_m\right]}{\mu_m\left[(1-c)\mu_m(1-2\nu_i)+\mu_i(1+c-2c\nu_m)\right]}\right]}{(1-2\nu)\left[\frac{b}{\ell}\left(I_0\left(\frac{b}{\ell}\right)+I_2\left(\frac{b}{\ell}\right)\right) - 2\left(I_2\left(\frac{b}{\ell}\right)+\nu I_1\left(\frac{b}{\ell}\right) - 2\nu I_2\left(\frac{b}{\ell}\right)\right)\right]} \tag{4.25}$$

$$c_{7\_3} = \frac{-4p\left[I_2\left(\frac{b}{\ell}\right)+\nu I_1\left(\frac{b}{\ell}\right) - 2\nu I_2\left(\frac{b}{\ell}\right)\right]\left[(1-2\nu) - \frac{\mu\left[(1+c)\mu_i(1-2\nu_m)+\mu_m(1-2\nu_i)(1-c-2\nu_m\right]}{\mu_m\left[(1-c)\mu_m(1-2\nu_i)+\mu_i(1+c-2c\nu_m)\right]}\right]}{(1-2\nu)\left[\frac{b}{\ell}\left(I_0\left(\frac{b}{\ell}\right)+I_2\left(\frac{b}{\ell}\right)\right) - 2\left(I_2\left(\frac{b}{\ell}\right)+\nu I_1\left(\frac{b}{\ell}\right) - 2\nu I_2\left(\frac{b}{\ell}\right)\right)\right]} \tag{4.26}$$

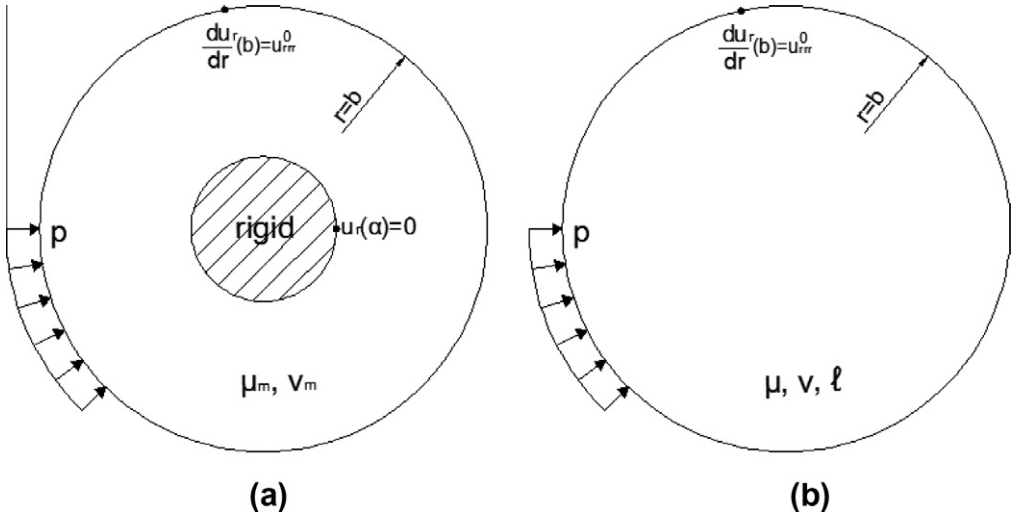

Fig. 7. Homogenization procedure of a material containing rigid inclusions: (a) Heterogeneous Cauchy material; (b) Homogeneous gradient material.

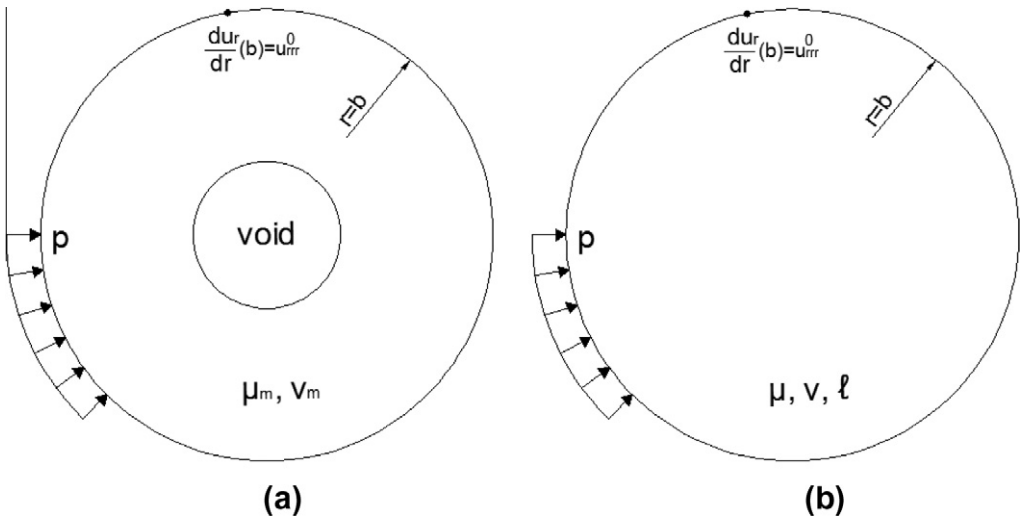

Fig. 8. Homogenization procedure of a porous material: (a) Heterogeneous Cauchy material; (b) Homogeneous gradient material.

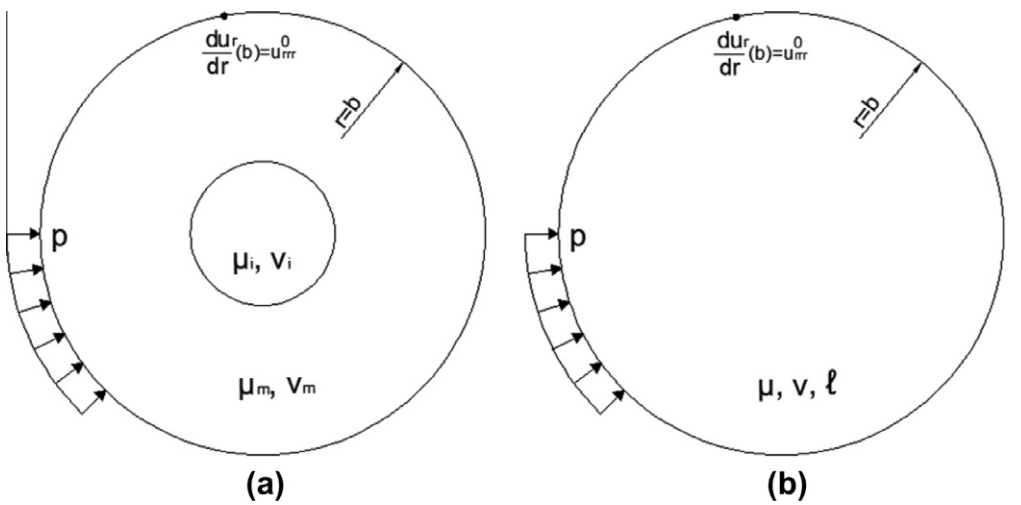

Fig. 9. Homogenization procedure of a material containing elastic inclusions: (a) Heterogeneous Cauchy material; (b) Homogeneous gradient material.

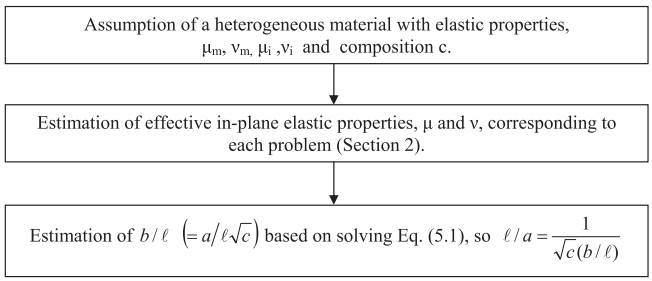

Fig. 10. Iteration process to estimate the internal length as a function of the composition, *c*, and the inclusion radius, *a*.

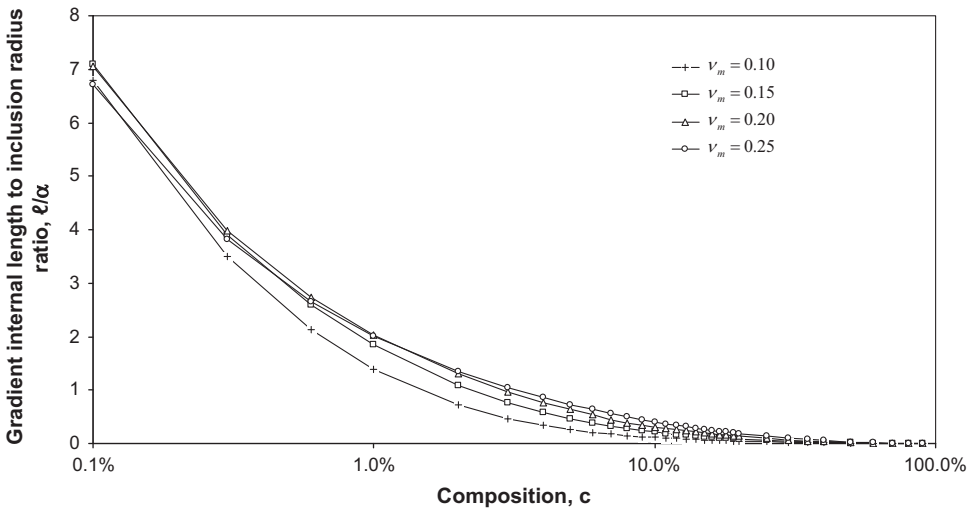

Fig. 11. Variation of the gradient internal length to the inclusion radius ratio ℓ/α, with respect to the composition *c*, for the case of rigid cylindrical inclusions.

Table 1
Variation of the normalized gradient internal length for the case of rigid inclusions.

c	b/ℓ				ℓ/α[a]			
	$\nu_m = 0.1$	$\nu_m = 0.15$	$\nu_m = 0.2$	$\nu_m = 0.25$	$\nu_m = 0.1$	$\nu_m = 0.15$	$\nu_m = 0.2$	$\nu_m = 0.25$
0.1%	4.6	4.5	4.5	4.7	6.802	7.088	7.058	6.707
1%	7.2	5.4	4.9	5.0	1.390	1.844	2.028	2.017
5%	17.1	9.6	7.0	6.1	0.262	0.468	0.640	0.732
10%	27.8	14.7	10.2	7.8	0.114	0.214	0.309	0.408
20%	47.9	26.4	16.7	12.0	0.047	0.085	0.134	0.186
30%	71.7	42.0	26.7	18.6	0.025	0.043	0.068	0.098
40%	106.2	66.1	43.1	29.6	0.015	0.024	0.037	0.053
50%	163.0	107.3	72.3	50.0	0.009	0.013	0.020	0.028
60%	268.2	186.3	130.2	91.7	0.005	0.007	0.010	0.014
70%	495.5	362.2	263.6	191.0	0.002	0.003	0.005	0.006
80%	1140.7	875.8	664.8	498.6	0.001	0.001	0.002	0.002
90%	4583.1	3685.0	2921.5	2277.0	0.000	0.000	0.000	0.000

[a] For the 2D case, the composition is: $c = a^2/b^2$.

schematically in Fig. 10. Throughout the calculations, a 5-digit accuracy was maintained. The numerical integration of the curves presented below converges as the interpolation order is increased.

5.1. Rigid inclusions

Estimation for the internal length for rigid inclusions is derived by equating the two associated energies, $U_{cl1} = U_{gr1}$

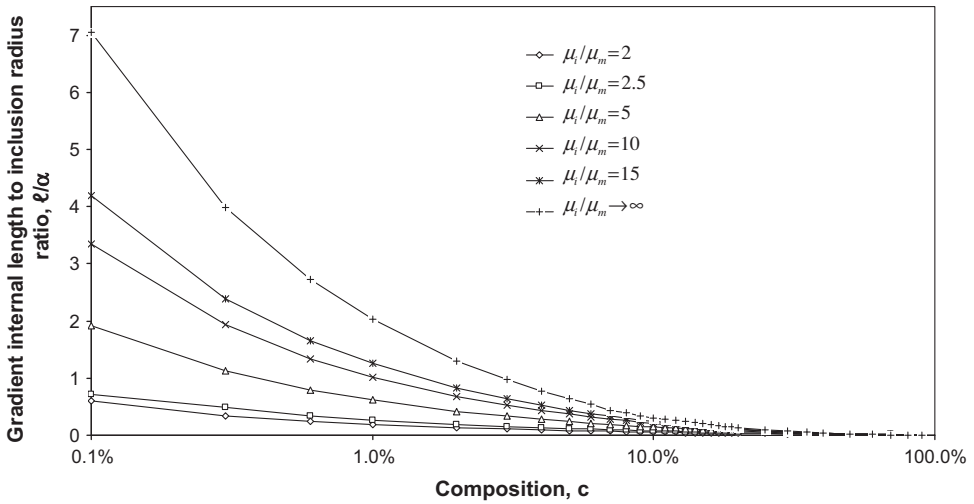

Fig. 12. Variation of the gradient internal length divided by the inclusion radius with respect to the composition c for the case of elastic cylindrical inclusions ($\nu_m = 0.2, \nu_i = 0.25$).

Table 2
Variation of the normalized gradient internal length for the case of elastic inclusions.

c	b/ℓ[a]					ℓ/α[b]				
	$\mu_i/\mu_m = 2$	$\mu_i/\mu_m = 2.5$	$\mu_i/\mu_m = 5$	$\mu_i/\mu_m = 10$	$\mu_i/\mu_m = 15$	$\mu_i/\mu_m = 2$	$\mu_i/\mu_m = 2.5$	$\mu_i/\mu_m = 5$	$\mu_i/\mu_m = 10$	$\mu_i/\mu_m = 15$
0.1%	52.5	44.1	16.6	9.4	7.5	0.602	0.717	1.909	3.350	4.193
1%	55.5	36.8	16.4	9.8	8.0	0.180	0.272	0.611	1.018	1.252
5%	54.6	38.5	18.6	12.0	10.2	0.082	0.116	0.240	0.372	0.440
10%	57.3	41.7	21.8	15.0	13.1	0.055	0.076	0.145	0.210	0.241
20%	64.3	49.4	29.4	22.4	20.3	0.035	0.045	0.076	0.100	0.110
30%	72.5	58.9	39.6	32.5	30.5	0.025	0.031	0.046	0.056	0.060
40%	82.5	70.7	54.0	47.9	46.1	0.019	0.022	0.029	0.033	0.034
50%	93.9	85.4	74.9	72.4	72.0	0.015	0.017	0.019	0.020	0.020
60%	106.7	103.5	106.0	113.6	117.7	0.012	0.012	0.012	0.011	0.011
70%	121.2	125.4	153.1	187.4	205.7	0.010	0.010	0.008	0.006	0.006
80%	136.4	152.1	227.2	332.6	398.5	0.008	0.007	0.005	0.003	0.003
90%	164.5	185.9	–	674.2	938.2	0.006	0.006	–	0.002	0.001

[a] The Poisson ratio of the matrix and inclusion is 0.2 and 0.25, respectively.
[b] For the 2D case, the composition is: $c = a^2/b^2$.

(see Fig. 7). The variation of the gradient internal length, ℓ, normalized by the radius of the inclusion,a, with the composition ratio c is shown in Fig. 11 in a semi logarithmic plot for ν_m values of 0.1, 0.15, 0.2 and 0.25. The results are also presented in Table 1. We note that the internal length increases with the matrix Poisson ratio.

5.2. Elastic inclusions

Estimation for the internal length for the case of elastic inclusions is derived by equating the two associated energies, $U_{cl3} = U_{gr3}$ (see Fig. 9). The variation of the gradient internal length, ℓ, normalized by the radius of the inclusion, α, with the composition ratio c is shown in Fig. 12 in a semi logarithmic plot for inclusion to matrix shear modulus ratio, μ_i/μ_m values of 2, 2.5, 5, 10 and 15 ($\nu_m = 0.2, \nu_i = 0.25$). For comparison purposes, the rigid case with $\nu_m = 0.2$ is plotted as well. These results are also presented in Table 2. The rigid inclusion case $\mu_i/\mu_m \to \infty$ gives the upper bound of ℓ/α and ℓ/α increases monotonically with $\mu_i/\mu_m > 1$. The internal length ℓ/α is a decreasing function of composition c, with $\ell/\alpha \to 0$ as $c \to 1$, as expected. It is noted that in all cases, when $c \to 0$, $\ell/\alpha \to \infty$ with $\int_0^1 \ell/\alpha dc$ finite. Note also that when the ratios μ_i/μ_m and ν_i/ν_m was assumed to be equal to one, no physically meaningful prediction was recovered from the problem as it should, because this case is essentially the case of a homogeneous material. The same was found to be true when the inclusion is less stiff than the matrix.

5.3. Porous material

Estimation for the internal length for the case of voids is derived by equating the two associated energies,

$U_{cl2} = U_{gr2}$, (see Fig. 8). The normalized internal length (b/ℓ) estimate for this case is of the order 10^{-8}, for the majority of c values, and for some values of c the estimate of b/ℓ becomes negative. These results can not be acceptable since they lack physical justification. In other words, there can be no realistic prediction for the internal length for the case of porous materials or generally when the inclusions are less stiff than the matrix. When inclusions are less stiff than the matrix, the micro-structural load path changes and strain gradient theories may be no longer applicable because microstructure with voids introduces gradients mostly in the antisymmetric part (rotations) than in the symmetric part (strains) of the deformations gradient. This is in agreement with Bigoni and Drugan (2007) who used a couple-stress (constaint Cosserat) model that emphasize on the rotation gradient. They proved that there can be no prediction for the microstructural length when particles are stiffer than the matrix. We could argue that the present results are complementary to those of Bigoni and Drugan (2007).

6. Remarks

6.1. Micromechanical explanation of the results

The predictions presented in Section 5 showed that as the composition is increased, the internal length estimates decreases. The internal length is associated with the microstresses that develop due to the microstructure of the composite. However when composition increases the distance between particles, decreases. Instead of having an inclusion embedded in a continuum, the problem resembles that of a particle with a thin layer around it. It has been shown (Budiansky and Carrier, 1984) that when this happens, the strain gradients reduce drastically.

6.2. Influence of the loading system

The estimates of Section 5 were based on an axisymmetric type of loading. In order to verify that these predictions hold true for other loading cases, we considered a different loading system that removes this symmetry. The second loading case corresponds to a remote uniaxial tension and the details of the solutions are presented in Appendix A. We consider the limiting case of rigid inclusions only and found that the material length prediction obtained from both loading cases is the same.

7. Application to fiber-reinforced concrete

A hooked end steel fiber reinforced concrete mixture (Papatheocharis, 2007) used currently by Lafarge for retrofitting structures has the following properties: $E_m = 40$ GPa, $v_m = 0.2$, $E_i = 210$ GPa, $v_i = 0.3$ and $c = 0.8\%$. The fibers have a circular cross section and the diameter is 5 mm. The shear modulus ratio of fibers and matrix is: $\mu_i/\mu_m = 4.85$. The density of the matrix is $\rho_m = 2350$ kg/m^3 and the density of the inclusion/fiber is $\rho_i = 7850$ kg/m^3

In order to obtain the estimate of the internal length, one can use either the assumption of elastic or rigid inclusion. The internal length estimate for each case is:

Rigid fiber assumption $\rightarrow \ell/a = 2.3 \Rightarrow \ell = 5.75$ mm
Elastic fiber assumption $\rightarrow \ell/a = 0.6 \Rightarrow \ell = 1.50$ mm

It is noted that this specific fiber-reinforced mixture was designed to be used as an outside jacket to existing reinforced concrete column and this jacket has typically a thickness between 3 cm and 5 cm.

7.1. Ben–Amoz estimate of the internal length parameter

The Ben–Amoz model (Ben-Amoz, 1976) for predicting the internal length parameter is based on a dynamic analysis of the micro and macro-structure. It is noted that in the absence of the dynamic conditions imposed on problem, the validity of model becomes questionable. Nevertheless, the Ben–Amoz model is the only other model in the literature that predicts the strain gradient internal length parameter and for this reason it is interesting to compare the two predictions. The key points of the model are presented below.

A normalized scale parameter, L/d, is introduced which can be seen as a measure of the strength of inhomogeneity. It is noted that this scale parameter is derived by assuming that the strain energy and kinetic energy are of the same order of magnitude but this assumption however is not always true.

The normalized scale parameter is:

$$L/d = \left[\rho_v(\lambda+2\mu)_v/\rho_R(\lambda+2\mu)_R\right]^{1/2} \tag{7.1}$$

where, $d = 2b$ for the 2D case.and subscripts v and R denote the Voigt and Reuss averaging quantities respectively, which are defined as follow:

$$\begin{aligned} ()_v &= c_m()_m + c_i()_i \\ \frac{1}{()_R} &= \frac{c_m}{()_m} + \frac{c_i}{()_i} \end{aligned} \tag{7.2}$$

where c is volume fraction and subscript m and i denotes the matrix and inclusion/fiber material.

The internal length parameters, ℓ_1 and ℓ_2, of Midlin's work for the long wave-length approximation (Mindlin, 1964, pp.69) are then associated with the scale parameter L by the following equations for the shear and dilatation modes:

$$\begin{aligned} \ell_1^2 &= \frac{L^2}{4}\left[1 - \frac{\mu_i - \mu_m}{\mu_v}(c_i - 4I_i)\right] \\ \ell_2^2 &= \frac{L^2}{4}\left[1 - \frac{(\lambda+2\mu)_i - (\lambda+2\mu)_m}{(\lambda+2\mu)_v}(c_i - 4I_i)\right] \end{aligned} \tag{7.3}$$

where for the 2D case $I_i = (a/b)^4 = c_i^2$

By applying the simplifications of the simplified strain gradient theory used throughout in this paper (see Mindlin, 1964, pp. 73, $\widehat{a}_1 = \widehat{a}_3 = \widehat{a}_5 = 0$, $\widehat{a}_2 = (\lambda/2)\ell^2$ and $\widehat{a}_4 = \mu\ell^2$), the Mindlin's internal length parameters become $\ell_1 = \ell_2 = \ell$. Hence, the Ben–Amoz model gives two different estimates for the internal length parameter,

which however for small values of the composition c are approximately the same. The Ben–Amoz predictions, for the specific fiber reinforced concrete mixture considered here, are:

Shear mode $\rightarrow \ell/a = 11.28 \Rightarrow \ell = 28.2$ mm
Dilatation mode $\rightarrow \ell/a = 11.22 \Rightarrow \ell = 28.05$ mm

8. Conclusions

The homogenization of a plane-strain heterogeneous Cauchy-elastic material was performed and the internal length parameter used in strain gradient theory was estimated for the cases of elastic inclusion stiffer than the matrix. Upper bound estimates for the internal length were found when inclusions much stiffer than the matrix were considered. The internal length was found to be between 0.5 and 7 times the inclusion radius for very small values of $c(c \cong 0.1\%)$ depending on the inclusion to matrix shear modulus ratio. The internal length decreases rather rapidly as the composition is increased and is approximately zero for $c > 70\%$. No prediction was possible for inclusions less stiff than the matrix and for the extreme case which corresponds to porous materials.

Acknowledgments

The current work is part of the "Hrakleitos II" project of the Greek Ministry of National Education for basic research on size effect phenomena. The authors would also like to thank Professor F. Perdikaris for his useful comments and Professor N. Aravas for sharing his findings.

Appendix A. Remote uniaxial tension case

We consider the problem of a circular inclusion of radius a inserted into an infinite isotropic body under remote uniaxial tension P as shown in Fig. A.1.

The plain-strain gradient solution for the radial and angular displacements outside the inclusion has been produced by Aravas (Private communication):

$$u_r(r,\theta) = \begin{cases} \frac{P}{4\mu} r(1-2\nu+\cos(2\theta)) \\ +\frac{P}{\mu}\left\{ \begin{array}{l} \left[A_1 \frac{a}{r} + A_3 \frac{a}{r} + A_5 \frac{a}{\ell} K_1\left(\frac{r}{\ell}\right)\right] \\ +\left[A_1 \frac{a}{r} + A_2 \frac{\ell}{r} K_2\left(\frac{r}{\ell}\right) + A_4 \left(\frac{a}{r}\right)^3 \right. \\ \left. +A_6\left(\frac{a}{r} K_2\left(\frac{r}{\ell}\right) + \frac{a}{2\ell} K_1\left(\frac{r}{\ell}\right)\right)\right] \cos(2\theta) \end{array} \right\} \end{cases} \tag{A.1}$$

$$u_\theta(r,\theta) = \begin{cases} -\frac{P}{4\mu} r \sin(2\theta) \\ +\frac{P}{\mu}\left\{ -\frac{1-2\nu}{2(1-\nu)} A_1 \frac{a}{r} + A_2\left(\frac{\ell}{r} K_2\left(\frac{r}{\ell}\right) + \frac{1}{2} K_1\left(\frac{r}{\ell}\right)\right) \right. \\ \left. +A_4\left(\frac{a}{r}\right)^3 + A_6 \frac{a}{r} K_2\left(\frac{r}{\ell}\right) \right\} \sin(2\theta) \end{cases} \tag{A.2}$$

where A_i ($i = 1..6$) are unknown coefficients.

The classical expressions of the displacements outside the inclusion for the case of rigid inclusions (Kachanov et al., 2003) are:

$$u_r^0(r,\theta) = \frac{Pa}{8\mu}\left\{ \left[(\upsilon-1)\frac{r}{a} + 2\gamma\frac{a}{r}\right] + \left[2\frac{r}{a} + \beta(\upsilon+1)\frac{a}{r} + 2\delta\left(\frac{a}{r}\right)^3\right]\cos(2\theta)\right\} \tag{A.3}$$

$$u_\theta^0(r,\theta) = \frac{Pa}{8\mu}\left\{ -2\frac{r}{a} - \beta(\upsilon+1)\frac{a}{r} + 2\delta\left(\frac{a}{r}\right)^3\right\}\sin(2\theta) \tag{A.4}$$

where $\beta = -2/\upsilon$, $\gamma = (1-\upsilon)/2$, $\delta = 1/\upsilon$ and $\upsilon = 3 - 4\nu$.

Note that both the gradient and classical solutions have the same dependence on the angle θ.

We demand that at $r = a$ and $r = b$ ($b > a$), the gradient displacements to be equal to the classical prediction:

$$\begin{aligned} u_r(a,\theta) &= u_r^0(a,\theta) \forall\theta \\ u_\theta(b,\theta) &= u_\theta^0(b,\theta) \forall\theta \end{aligned} \tag{A.5}$$

Eq. (A.5) describe a system of six equations that can be solved for the six unknowns A_i. The coefficients that become zero are:

$$A_2 = A_5 = A_6 = 0 \tag{A.6}$$

Therefore, the gradient solution reduces to the classic solution but this however does not mean that the gradient effect disappears as in the case of axisymmetric loading. In essence we apply the same kinematic admissible field to the gradient homogeneous material and classic

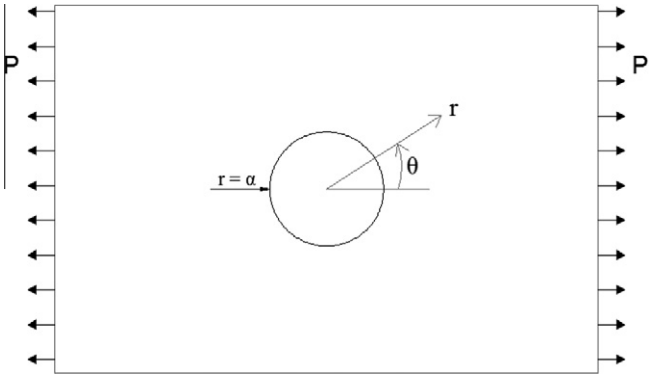

Fig. A.1. Inclusion of radius a inserted into an infinite body under uniaxial tension P.

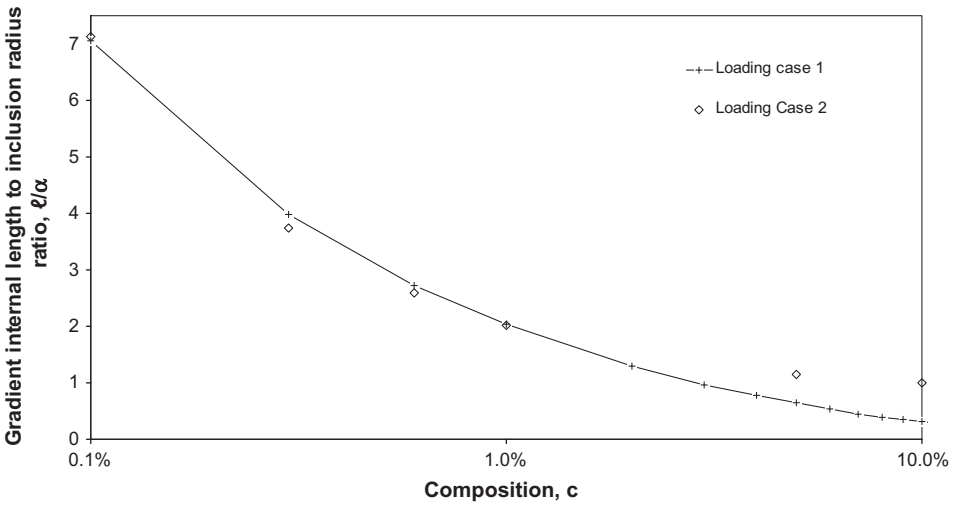

Fig. A.2. Variation of the gradient internal length to the inclusion radius ratio ℓ/α, with respect to the composition c, for the case of rigid cylindrical inclusions, obtained for two different loading cases ($\nu_m = 0.2$).

heterogeneous material. Therefore, the boundary conditions for the two systems at $r = a$ and $r = b$ are the same. Obviously, this kinematic field is the same only for $r \geqslant a$, but for the case of dilute composites ($a << b$), the total elastic energy calculated for $b \geqslant r \geqslant a$ is approximately the same with the total elastic energy calculated for $b \geqslant r \geqslant 0$.

The expression for the total elastic energy for the heterogeneous classic material is:

$$U_{cl} = 4\int_0^{\pi/2}\int_a^b \frac{1}{2} r(\tau_{rr}\varepsilon_{rr} + \tau_{\theta\theta}\varepsilon_{\theta\theta} + 2\tau_{r\theta}\varepsilon_{r\theta})drd\theta \tag{A.7}$$

The expression of the total elastic energy for the homogeneous gradient material is:

$$U_{gr} = 4\int_0^{\pi/2}\int_\alpha^b \frac{1}{2} r\begin{pmatrix} \tau_{rr}\varepsilon_{rr} + \tau_{\theta\theta}\varepsilon_{\theta\theta} + 2\tau_{r\theta}\varepsilon_{r\theta} \\ +\lambda_{rrr}k_{rrr} + \lambda_{r\theta\theta}k_{r\theta\theta} + 2\lambda_{rr\theta}k_{rr\theta} \\ +\lambda_{\theta rr}k_{\theta rr} + \lambda_{\theta\theta\theta}k_{\theta\theta\theta} + 2\lambda_{\theta r\theta}k_{\theta r\theta} \end{pmatrix} drd\theta \tag{A.8}$$

It is reminded that the double stress λ and the third order strains k are defined by Eq. (4.3) accounting that:

$$\begin{aligned} \nabla &= \mathbf{e}_r\frac{\partial}{\partial r} + \mathbf{e}_\theta\frac{1}{r}\frac{\partial}{\partial\theta}, \\ \nabla\tau &= \tfrac{\partial\tau_{rr}}{\partial r}\mathbf{e}_{rrr} + \tfrac{\partial\tau_{\theta\theta}}{\partial r}\mathbf{e}_r\mathbf{e}_\theta\mathbf{e}_\theta + \tfrac{\partial\tau_{r\theta}}{\partial r}\mathbf{e}_r(\mathbf{e}_r\mathbf{e}_\theta + \mathbf{e}_\theta\mathbf{e}_r) \\ &\quad + \tfrac{1}{r}\left(\tfrac{\partial\tau_{rr}}{\partial\theta} - 2\tau_{r\theta}\right)\mathbf{e}_\theta\mathbf{e}_r\mathbf{e}_r + \tfrac{1}{r}\left(\tfrac{\partial\tau_{\theta\theta}}{\partial\theta} + 2\tau_{r\theta}\right)\mathbf{e}_\theta\mathbf{e}_\theta\mathbf{e}_\theta \\ &\quad + \tfrac{1}{r}\left(\tfrac{\partial\tau_{r\theta}}{\partial\theta} + \tau_{rr} - \tau_{\theta\theta}\right)\mathbf{e}_\theta(\mathbf{e}_r\mathbf{e}_\theta + \mathbf{e}_\theta\mathbf{e}_r) \end{aligned} \tag{A.9}$$

where **e** is the base vector.

Under the assumption of dilute composition, we can demand equality of the two energies since both systems have the same boundary conditions and the gradient energy part neglected i.e. $\alpha \geqslant r \geqslant 0$ is very small if $b >> \alpha$, i.e. $c << 1$. The other two material properties, i.e. in-plane shear modulus and Poisson ratio for the gradient material are again extracted from the Cristensen predictions (see Section 2).

The variation of the gradient internal length, ℓ, normalized by the radius of the inclusion, α, with the composition ratio c is shown in Fig. A.2 for the case of rigid inclusions and assuming that the matrix Poisson ratio is $\nu_m = 0.2$. The solid line corresponds to the loading case 1 (see Fig. 7) and the diamond symbols correspond to loading case 2 (see Fig. A.1). The prediction for the second loading case was derived under the assumption of dilute concentration of inclusions and hence we plot only the predictions for $c < 10\%$. As can be seen in Fig. A.2, the match between the two estimates is very good at low values of c and as c increases the two predictions differ as expected since the dilute composition assumption is compromised. Nevertheless, the results clearly show that a different loading system did not affect the prediction of the internal length parameter.

References

Abramowitz, M., Stegun, A.I., 1970. Handbook of Mathematical Functions, 7th ed. Dover Publications, INC., New York.
Aravas, N., 2011. Plane-stain problems for a class of gradient elasticity models-a stress function approach. J. Elast. 45, 100–110.
Aravas N. Private communication.
Ben-Amoz, M., 1976. A dynamic theory for composite materials. J Appl. Math. Ph. (ZAMP) 27, 83–99.
Bigoni, D., Drugan, W.J., 2007. Analytical derivation of Cosserat moduli via homogenization of heterogeneous materials. J. App. Mech. 74, 741–753.
Budiansky, B., 1965. On the elastic moduli of some heterogeneous materials. J. Mech. Phys. Solids 13, 223–227.
Budiansky, B., Carrier, G.F., 1984. High shear stresses in stiff fiber composites. J. Appl. Mech. 51, 733–735.
Christensen, M.R., 1990. A critical evaluation for a class of micro-mechanics models. J. Mech. Phys. Solids 38, 379–404.
Christensen, R.M., Lo, K.H., 1979. Solution for the effective shear properties in three phase sphere and cylindrical models. J. Mech. Phys. Solids 27, 315–330, Erratum 34: 639.
Eshel, N.N., Rosenfeld, G., 1975. Axi-symmetric problems in elastic materials of grade two. J. Franklin Institute 299, 43–51.
Eshelby, J.D., 1957. The determination of the elastic field of an ellipsoidal inclusion, and related problems. Proc. R. Soc. A241, 376–396.

Gao, X.L., Park, S.K., 2007. Variational formulation of a simplified strain gradient elasticity theory and its application to a pressurized thick-walled cylinder problem. Int. J. Solids Stuct. 44, 7486–7499.
Hashin, Z., Rosen, B.W., 1964. The elastic moduli of fiber-reinforced materials. J. Appl. Mech. 31, 223–232.
Hill, R., 1965. A self-consistent mechanics of composite materials. J. Mech. Phys. Solids 13, 213–222.
Kachanov, M., Shafiro, B., Tsukov, I., 2003. Handbook of Elasticity Solutions. Kluwer Academic Publishers, Dordrecht.
Koiter WT. Couple-stresses in the theory of elasticity. Part I, In: Proceedings of Ned. Akad. Wet. B67, 17-29:II 1964, pp. 30–44.
McLaughlin, R., 1977. A study of the differential scheme for composite materials. Int. J. Eng. Sci. 15, 237–244.
Mindlin, R.D., 1964. Micro-structure in linear elasticity. Arch. Ration. Mech. Anal. 16, 51–78.
Mindlin, R.D., Tiersten, H.F., 1962. Effects of couple-stresses in linear elasticity. Arch. Ration. Mech. Anal. 11, 415–448.
Mori, T., Tanaka, K., 1973. Average stress in matrix and average elastic energy of materials with misfitting inclusions. Acta Metall. 21, 571–574.
Norris, A.N., 1985. A differential scheme for the effective moduli of composites. Mech. Metall. 21, 1–16.
Papatheocharis T. Experimental study of fiber-reinforced concrete beams response to static and cyclic bending, MSc Thesis, University of Thessaly, Dept. of Civil Engineering, Volos, Greece, 2007.
Timoshenko, S., Goodier, J.N., 1951. Theory of Elasticity, 2nd ed. McGraw-Hill Book Company, New York.
Toupin, R.A., 1962. Perfectly elastic materials with couple stresses. Arch. Ration. Mech. Anal. 11, 385–414.